Short-circuit boundary conditions in ferroelectric $PbTiO_3$ thin films

Alexie M. Kolpak, Na Sai, and Andrew M. Rappe*
The Makineni Theoretical Laboratories, Department of Chemistry, University of Pennsylvania, 231 South 34th Street, Philadelphia, Pennsylvania 19104-6323, USA

(Received 27 December 2005; revised manuscript received 23 May 2006; published 29 August 2006; corrected 1 September 2006)

We examine the application of short-circuit electrical boundary conditions in density-functional theory calculations of ferroelectric thin films. Modeling $PbTiO_3$ films with metallic electrodes, we demonstrate that under periodic boundary conditions of supercells, short-circuit conditions for the electrodes are equivalently satisfied in two repeated slab geometries: a $PbTiO_3$/metal superlattice geometry and a periodic metal/$PbTiO_3$/metal/vacuum geometry, where the metal is Pt or $SrRuO_3$. We discuss the benefits of each geometry in the study of ferroelectricity in thin films.

DOI: 10.1103/PhysRevB.74.054112 PACS number(s): 77.80−e, 77.22.Ej, 71.15.−m

The application of relevant electrostatic boundary conditions in first-principles simulations of ferroelectric thin films is extremely important.[1–5] In many studies, the calculations are carried out on systems composed of a ferroelectric thin film sandwiched between two metal electrodes in short-circuit conditions,[6,7] i.e., the electrostatic potential through both electrodes is the same. The short-circuit boundary conditions are also relevant to most experiments.[8]

Under supercell periodic boundary conditions in the first-principles studies, one way to satisfy the short-circuit conditions is to consider a slab geometry consisting of repeated ferroelectric/metal units, in which the metal layers are thick enough so that copies of the ferroelectric film do not interact with each other.[4] In this geometry, illustrated schematically in Fig. 1(a), the short-circuit boundary conditions are directly enforced, with contact between the metal electrodes at the top and bottom of the ferroelectric film through a bulklike region of the metal. In this case, the entire ferroelectric/electrode structure can be relaxed by considering the unit cell strain as a variational parameter.

It is also possible to model ferroelectric thin films using an isolated capacitor geometry that contains electrode/ferroelectric/electrode slabs that are separated by vacuum, such as in Fig. 1(b). This geometry is computationally less efficient than the continuous geometry (requiring more atoms and larger supercells), but it is beneficial in that there is no artificial constraint on the unit cell strains along the surface normal direction, and therefore no need to rely on the strains to find the relaxed geometry. By separating the effects of the positive and negative ferroelectric surface charges on the metal behavior, an isolated geometry also facilitates the study of work functions at the ferroelectric surface[3] and the comparison of complete and partial screening in thin metal films. Furthermore, this arrangement is useful for studying the effects of having different top and bottom electrodes, since it eliminates the influence of an additional interelectrode interface. However, unlike in the continuous geometry, it is not obvious whether the necessary electrostatic boundary conditions can be achieved in an isolated structure.

In this paper, we demonstrate using density-functional theory (DFT) calculations that short-circuit boundary conditions are satisfied in both continuous and isolated geometries. We determine the minimum electrode thickness in each geometry for ultrathin ferroelectric $PbTiO_3$ (001) films with platinum (Pt) and $SrRuO_3$ electrodes, and we demonstrate that, given sufficiently thick electrodes, the desired electrostatic boundary conditions are satisfied in both geometries. Furthermore, we show that with electrodes at or above the minimum thickness, the ferroelectric structure of the perovskite films, as well as the electronic behavior of both the metallic and perovskite regions, is indistinguishable in the two geometries.

Our calculations were performed using DFT with the generalized gradient approximation as implemented in the *ab initio* code DACAPO,[12] with a plane wave cutoff of 30 Ry and a $4\times4\times1$ Monkhorst-Pack k-point mesh,[9] and all calculations correspond to $T=0$ K. The $PbTiO_3$ structures considered consist of five atomic layers, three layers of TiO_2 sepa-

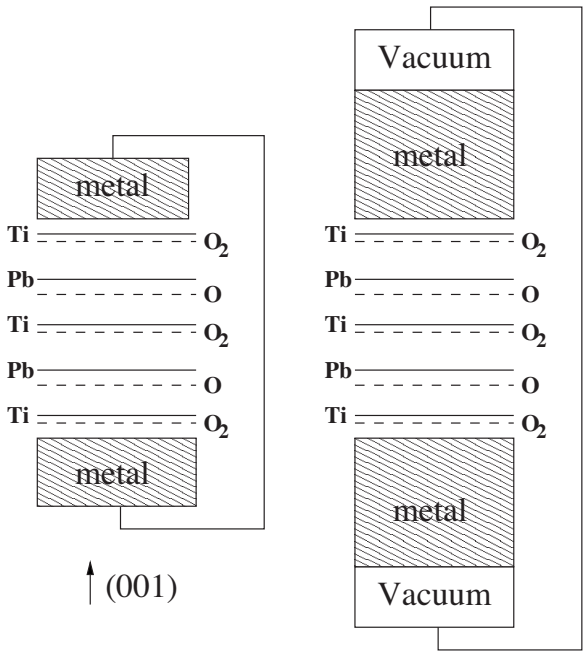

FIG. 1. Schematic of $PbTiO_3$ in the continuous (left) and isolated (right) geometries. Periodic slabs in the former are in contact to form a continuous lattice, while in the latter the slabs are separated by a large vacuum. The horizontal solid and dashed lines indicate the relaxed positions of the cations and oxygens, respectively, in the film surface normal direction.

rated by PbO planes stacked in the (001) direction, as illustrated by the schematic in Fig. 1. Experimentally, cubic $SrTiO_3$ and tetragonal $PbTiO_3$ have the same in-plane lattice constant (3.905 Å), so the interface is stress free. To model stress-free growth of tetragonal $PbTiO_3$ on $SrTiO_3$, the in-plane lattice constant was fixed to the theoretical equilibrium bulk value of 3.86 Å. All atomic coordinates were fully relaxed until the forces on each atom are less than 0.01 eV/Å. Polarization is perpendicular to the interface, which is energetically favorable for this choice of in-plane lattice constant.[13] The interfacial Pt atoms are in the energetically favored positions above the TiO_2 oxygens, and additional Pt layers continue the (001) lattice. In the continuous geometry, periodic copies of the $PbTiO_3$ film are separated by a Pt electrode of $l_{Pt}=3$, 5, 7, or 9 atomic layers,[14] while in the isolated geometry, the $PbTiO_3$ film is sandwiched between two Pt electrodes, each of thickness l_{Pt}, and the entire structure is then separated from its periodic images by 20 Å of vacuum. In the isolated geometry, a dipole correction[10] was applied in the center of the vacuum region.

The ferroelectric behavior of the $PbTiO_3$ films can be characterized by the set of rumpling parameters, $\delta z = z_{Pb(Ti)} - z_O$, which describes the cation-oxygen separation along the polarization direction for each PbO and TiO_2 layer in a given film. In the continuous structures, we expect that δz will evolve as l_{Pt} increases, until the Pt thickness is sufficient to completely screen the two $PbTiO_3$ surfaces from each other. We expect the isolated geometry to behave similarly, with δz changing until the electrodes are thick enough to prevent interactions between each $PbTiO_3$ surface and the corresponding electrode/vacuum interfaces. Furthermore, we expect the converged δz values to be equal in the two geometries.

To determine the minimum electrode thickness for converged ferroelectric thin film properties, we consider the evolution of ferroelectric rumpling δ_z as a function of electrode thickness l_{Pt}. Table I gives the values for the continuous and isolated geometries, respectively, as a fraction of the bulk rumpling parameters. As the table shows, the ferroelectric behavior of the $PbTiO_3$ films with Pt electrodes is identical in the continuous and isolated geometries for structures with $l_{Pt} \geq 7$, with all atoms in the same positions to within <0.001 Å. Similarly, the $PbTiO_3$ rumpling profiles in the two geometries converge to a single structure with $SrRuO_3$ electrodes of nine or more layers. Table I shows that $PbTiO_3$ films with Pt electrodes have polarization enhanced by $\approx 15\%$ relative to bulk at the positive surface and decreased by slightly more at the negative surface, while the central layers of the film show bulklike rumpling. The δz values in films with $SrRuO_3$ electrodes are all smaller than the bulk values, giving a total polarization of approximately 30% of the bulk $PbTiO_3$ polarization. These smaller atomic displacements, as well as the smaller ferroelectric-paraelectric energy differences for films with $SrRuO_3$ electrodes (given in Table I), suggest that Pt electrodes are more effective at stabilizing perpendicular polarization in $PbTiO_3$ films.

In a grounded $PbTiO_3$/metal system, electrons are able to flow through the electrode(s) from one ferroelectric/electrode interface to the other, regardless of geometry. Consequently, an electric field cannot be sustained through the electrode,

TABLE I. Rumpling parameters δz for the continuous and isolated geometries as a fraction of the theoretical bulk rumpling parameters, $\delta z_{bulk}(TiO_2)=0.51$ Å and $\delta z_{bulk}(PbO)=0.87$ Å. The first TiO_2 layer corresponds to the bottom $PbTiO_3$ surface in Fig. 1, with the surface normal parallel to the polarization. The ferroelectric-paraelectric energy difference, $\Delta E = E_{ferro} - E_{para}$, is also shown, in units of eV. A negative value of ΔE indicates an energetically favorable ferroelectric state.

l_{Pt}	TiO_2	PbO	TiO_2	PbO	TiO_2	ΔE
Continuous						
3	0.82	0.88	0.93	0.93	1.14	−0.33
5	0.81	0.91	0.93	0.94	1.14	−0.27
7	0.82	0.95	0.96	0.98	1.16	−0.24
9	0.82	0.95	0.96	0.98	1.16	−0.24
Isolated						
3	0.83	0.95	0.97	0.99	1.17	−0.30
5	0.83	0.94	0.97	0.99	1.16	−0.24
7	0.82	0.95	0.96	0.98	1.16	−0.24
9	0.82	0.95	0.96	0.98	1.16	−0.24
l_{SrRuO_3}	TiO_2	PbO	TiO_2	PbO	TiO_2	
Continuous						
5	0.38	0.24	0.36	0.24	0.30	−0.09
7	0.36	0.22	0.35	0.22	0.29	−0.13
9	0.35	0.21	0.34	0.22	0.28	−0.14
11	0.36	0.21	0.33	0.22	0.28	−0.14
Isolated						
5	0.34	0.20	0.32	0.21	0.26	−0.01
7	0.35	0.21	0.35	0.22	0.27	−0.07
9	0.36	0.21	0.33	0.22	0.27	−0.14
11	0.36	0.21	0.33	0.22	0.28	−0.14

and therefore the electrostatic potential must be flat through the electrode region. Macroaveraging[3,4,11] the electrostatic potential in the continuous geometry, as illustrated in Fig. 2(a), shows that structures with electrodes of seven and nine atomic layers of Pt are indeed in short-circuit, with clear zero-slope regions through the center of the electrode. On the other hand, the structures with $l_{Pt}<7$ do not exhibit rigorously equipotential regions. As the potential for $l_{Pt}=3$ illustrates, the Pt regions corresponding to each interface meet, leaving no equipotential region. Increasing the Pt thickness to five layers allows separate Pt and interface regions to emerge, but a small electrostatic potential slope remains, demonstrating that $l_{Pt}=5$ is insufficient to completely prevent interactions between the periodic copies of the $PbTiO_3$ film. The small slope through the electrode for each l_{Pt} is given in the left side of Table II, quantitatively indicating the rapid decrease of the field with increasing electrode thickness. The zero slope through the electrode for films with $l_{Pt}>5$ confirms that these structures are in short-circuit.

The electrostatic potentials of $PbTiO_3$/Pt structures in the isolated geometry, plotted in Fig. 2(b), show a similar picture. As in the continuous geometry, it is not possible to

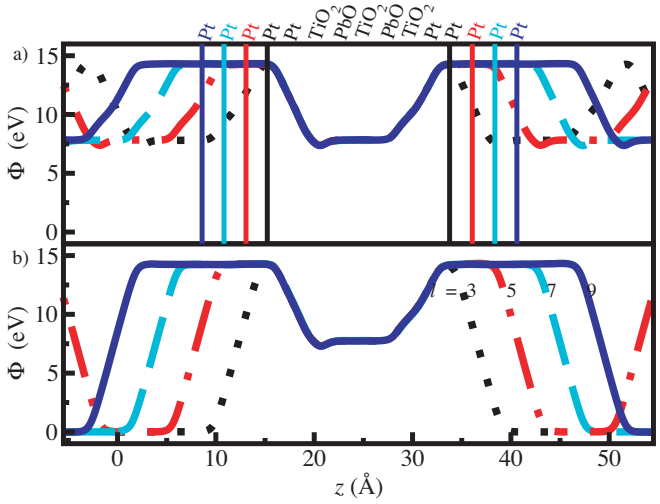

FIG. 2. (Color online) Layer-averaged electrostatic potentials, $\Phi(z)$, along (001) for structures in the (a) continuous and (b) isolated geometries. The curves for films with $l_{Pt}=3$, 5, 7, and 9 are shown with black dotted, red dot-dashed, cyan dashed, and blue solid lines, respectively. The vertical black, red, cyan, and blue lines in (a) bound a single repeat of the periodic supercell for $l_{Pt}=3$, 5, 7, and 9, respectively; the lines on the left side of the ferroelectric film are positioned at the central Pt layer for each l_{Pt} (labeled in the corresponding color), and those on the right mark the same Pt layer in the next supercell.

clearly differentiate the electrode from the interfaces for $l_{Pt}=3$. In addition, five Pt layers are again not thick enough to eliminate fields through the electrode due to the polarization charge, as shown by the nonzero value of the slope given in Table II. Most significantly, however, the potentials are again flat through the central region of the electrodes for the structures with $l_{Pt}>5$, suggesting that charge is successfully transferred between the two $PbTiO_3$/Pt interfaces. The magnitude of the dipole correction, p_{corr}, also reported in Table II, further indicates that the system is in short-circuit; p_{corr} goes to zero for $l_{Pt}>5$, as there is no net dipole through the Pt/$PbTiO_3$/Pt structure.

Figure 2 also shows that the field through the ferroelectric slab, E_{FE}, is very similar for all l_{Pt}, regardless of the geometry. The magnitude of the field through the central unit cell (the middle three layers in Fig. 1), reported in Table II, again indicates that the minimum electrode thickness for converged ferroelectric properties in both geometries is $l_{Pt}=7$.

Interestingly, the evolution of E_{FE} with $SrRuO_3$ thickness is dependent on the geometry, with E_{FE} decreasing towards the converged value in the continuous geometry, and increasing to the converged value in the isolated geometry. The difference in the trend demonstrates the importance of choosing electrodes of sufficient thickness in studying the behavior of charge passivation in ferroelectric/metal capacitors. The identical converged values of E_{FE}, however, show that the two geometries are equivalent once this condition is satisfied.

With $SrRuO_3$ electrodes, the field through the $PbTiO_3$ is significantly larger than that found with Pt electrodes. Nevertheless, as Table II shows, the evolution of the electrostatic potential as a function of electrode thickness is similar for both electrode materials. In the $PbTiO_3$/$SrRuO_3$ films, the slope through the ferroelectric converges to a value of 0.053 eV/Å and the field through the electrodes approaches zero as the $SrRuO_3$ thickness is increased to $l_{SrRuO_3}=11$, regardless of the film geometry. The larger minimum electrode thickness determined for the $PbTiO_3$/$SrRuO_3$ films reflects the longer screening length of $SrRuO_3$ compared to Pt.

TABLE II. Magnitude of the electric fields E_{metal} and E_{FE} through the electrode and ferroelectric regions, respectively, as a function of electrode thickness for continuous and isolated geometries. The values for E_{metal} in the isolated geometry show the average of the slope through the two electrodes. The magnitude of the dipole correction in the isolated geometry, p_{corr}, is also given, in units of Å. The electric fields, in units of V/Å, are determined from the macroaveraged (Ref. 11) electrostatic potentials by a linear fit to the central 4 Å in the $PbTiO_3$ films and the $SrRuO_3$ electrodes, and to the inner $l-2$ layers in the Pt electrodes. The uncertainty in the electric fields is ±0.0005 V/Å.

	Continuous		Isolated		
l_{Pt}	E_{Pt}	E_{FE}	E_{Pt}	E_{FE}	p_{corr}
3		0.0100		0.0031	0.007
5	0.0103	0.0006	0.0180	0.0006	0.003
7	0.0001	0.0004	0.0001	0.0003	0.001
9	0.0001	0.0003	0.0001	0.0003	0.000
l_{SrRuO_3}	E_{SrRuO_3}	E_{FE}	E_{SrRuO_3}	E_{FE}	p_{corr}
5	0.0350	0.0624	0.0838	0.0460	0.026
7	0.0029	0.0549	0.0160	0.0520	0.015
9	0.0001	0.0525	0.0002	0.0534	0.000
11	0.0001	0.0530	0.0001	0.0530	0.000

The above data demonstrate that for both electrode materials, charge transfer occurs between the two $PbTiO_3$/metal interfaces in the isolated geometry, despite the fact that the electrodes are not in direct contact. This is possible due to the nature of the computation, which requires that the electrodes are provided with electrons from a single reservoir; i.e., there is a constant chemical potential of electrons. Consequently, the minimum electrode thickness necessary to short-circuit the system is defined in the same manner as in the continuous geometry, as the thickness necessary to screen interactions between interfaces, in this case, the $PbTiO_3$/metal and metal/vacuum interfaces sandwiching each electrode.

Examination of the density of states (DOS) of the central metal layer offers further confirmation that short-circuit boundary conditions have been satisfied in both geometries. In grounded systems with electrodes of sufficient thickness to prevent interaction between periodic copies of the $PbTiO_3$ film, the electronic structure of the central metal layer should be identical to the corresponding layer in an (001) metal slab, as the effects of the ferroelectric film (or the vacuum) will be completely screened in this region. In Fig. 3, the *d*-band

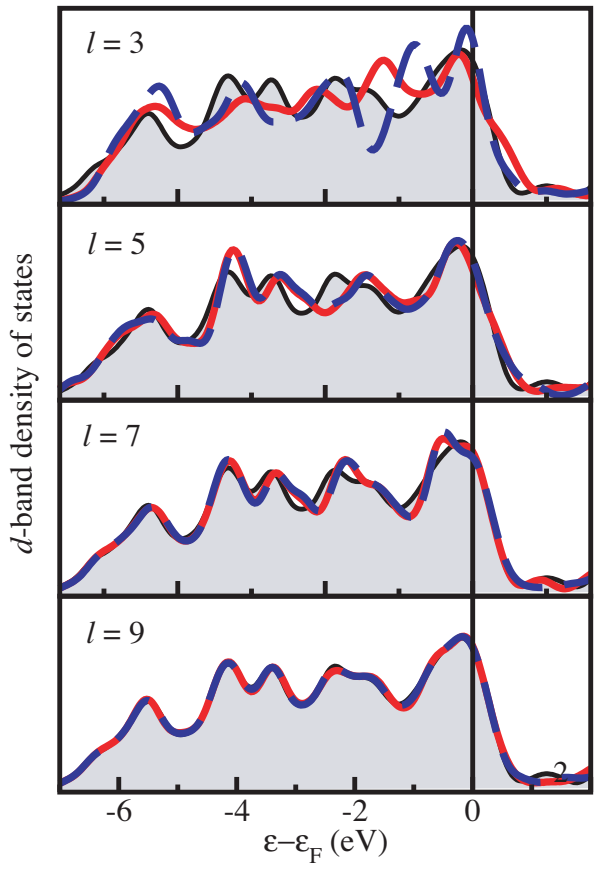

FIG. 3. (Color online) *d*-band DOS of the central Pt layer in the electrodes of the continuous (solid red curve) and isolated (dashed blue curve) geometries. In both geometries, the Pt DOS in the center of the nine-layer electrodes is virtually identical to that in the center of a thick Pt (001) slab (shaded).

DOS of $PbTiO_3$/Pt structures in the continuous and isolated geometries are compared to the DOS of the middle Pt layer in a nine-layer Pt (001) film with the same in-plane lattice constant. As the top panel of the figure shows, the *d*-band of the continuous (solid curve) and isolated (dashed curve) structures with $l_{Pt}=3$ differ significantly from the Pt (001) *d*-band (shaded). They also differ from each other, as expected from the structural data shown in Table I. As l_{Pt} is increased, the continuous and isolated *d*-bands look increasingly similar to that of the Pt (001). Although there are still minor differences between the DOS of the seven-layer structures and Pt (001), the isolated and continuous *d*-bands for the $l_{Pt}=9$ structures are both essentially indistinguishable from the Pt (001) *d*-band.

The DOS of the central layer in the $SrRuO_3$ electrodes, not shown due to space constraints, also becomes very similar to the corresponding SrO or RuO_2 layer in a thick $SrRuO_3$ slab as l_{SrRuO_3} increases, displaying only small differences for $l_{SrRuO_3} \geqslant 9$.

In conclusion, we have shown that short-circuit boundary conditions are satisfied in ferroelectric $PbTiO_3$/metal capacitor structures in two geometries when the electrode thickness is greater than five Pt layers or seven $SrRuO_3$ layers. We have shown that, for a given electrode material, the ferroelectric films in the continuous and isolated geometries converge to the same atomic structure, and that the potential in the ferroelectric and metal regions is identical for both geometries with electrodes of sufficient thickness, resulting in indistinguishable ferroelectric behavior. In such structures, the electrostatic potential has zero slope through the center of the metal electrode, demonstrating that electron transfer between the $PbTiO_3$/metal interfaces is accomplished, via direct contact between the electrodes in the continuous geometry or as a result of a single reservoir of electrons shared by the electrodes in the isolated geometry. An electronic structure analysis shows that the DOS of the central metal layer is almost identical to that in the corresponding metal slab, further demonstrating that these structures are in short-circuit. Our results demonstrate that ferroelectric capacitor structures can be accurately modeled in either geometry, allowing the possibility to utilize the benefits of both in further studies.

This work was supported by the Office of Naval Research under Grant No. N-000014-00-1-0372, the Center for Piezoelectric Design, and the National Science Foundation, through the MRSEC program, Grant No. DMR05-20020. Computational support was provided by the HPCMO and DURIP. A.M.K. was supported by Arkema Inc.

*Electronic address: rappe@sas.upenn.edu

[1] B. Meyer and D. Vanderbilt, Phys. Rev. B **63**, 205426 (2001).
[2] P. Ghosez and K. M. Rabe, Appl. Phys. Lett. **76**, 2767 (2000).
[3] N. Sai, A. M. Kolpak, and A. M. Rappe, Phys. Rev. B **72**, 020101(R) (2005).
[4] J. Junquera and P. Ghosez, Nature (London) **422**, 506 (2003).
[5] E. Almahmoud, N. Y. I. Kornev, H. X. Fu, and L. Bellaiche, Phys. Rev. B **70**, 220102(R) (2004).
[6] T. M. Shaw, S. Trolier-McKinstry, and P. C. McIntyre, Annu. Rev. Mater. Sci. **30**, 263 (2000).
[7] M. Dawber, K. M. Rabe, and J. F. Scott, Rev. Mod. Phys. **77**, 1083 (2005).
[8] K. M. Indlekofer and H. Kohlstedt, Europhys. Lett. **72**, 282 (2005).
[9] H. J. Monkhorst and J. D. Pack, Phys. Rev. B **13**, 5188 (1976).
[10] L. Bengtsson, Phys. Rev. B **59**, 12301 (1999).
[11] A. Baldereschi, S. Baroni, and R. Resta, Phys. Rev. Lett. **61**, 734 (1988).
[12] http://dcwww.camp.dtu.dk/campos/Dacapo/
[13] In fact, we find that perpendicular polarization is favored over in-plane polarization for $PbTiO_3$ in-plane lattice constants from 2.5% less than the equilibrium value up to 0.5% above the equilibrium lattice constant, at which point the in-plane polarization becomes more favorable. Since the Pt(100) lattice constant is

only 0.38% larger than that of $SrTiO_3$, we predict perpendicular polarization for $PbTiO_3$ grown on Pt(100). The in-plane polarization has been studied by I. Kornev *et al.* [Phys. Rev. Lett. **93**, 196104 (2004)] and by Meyer, Padilla, and Vanderbilt [Faraday Discuss. **114**, 395 (1999)]. Here we address the out-of-plane polarization while leaving the boundary conditions relating to in-plane polarization to a future study.

[14] We consider electrodes with an odd number of metal layers and a single middle layer, as required by the continuous geometry.